

Assessing environmental control on dinoflagellate cyst distribution in surface sediments of the Benguela upwelling region (eastern South Atlantic)

Frank-D. Bockelmann¹ and Karin A. F. Zonneveld

Department of Geosciences, Bremen University, P.O. Box 330440, D-28334 Bremen, Germany

Martin Schmidt

Baltic Sea Research Institute Warnemünde, Seestrasse 15, D-18119 Rostock, Germany

Abstract

Organic-walled dinoflagellate cyst assemblages in surface sediments of the Benguela Current Upwelling System (eastern South Atlantic) show geographic patterns that cannot entirely originate from cyst production or transport. Aimed at answering how far these variations are due to taphonomic control, this study investigated a possible correlation with the changes in bottom-water oxygen concentrations typifying this region. Based on 36 samples, multivariate statistics were used to analyze community variability with respect to bottom-water oxygen concentration, temperature, salinity, nutrient content, chlorophyll *a* (Chl *a*) concentration, the organic carbon content of surface sediments, and a measure of water column stratification. Determined relationships to salinity, nutrient supply, nutrition, and environmental steadiness point out the requirements for dinoflagellate cyst production, while cross-shelf transport processes could have introduced variability prior to burial of cysts in surface sediments. The offshore decrease in the relative abundance of protoperidiniacean cyst types was consistent with their lower preservation potential under oxygenated conditions and coincided with a change in assemblage composition toward oxidation resistant species. On elimination of covariation, bottom-water oxygenation was significantly related to this pattern and determined together with seasonal salinity, Chl *a*, and annual phosphate concentration, the parameter combination best explaining community variability. These results suggest that postdepositional degradation of peridinioid dinoflagellate cysts would partly explain the onshore–offshore gradient in species distributions and could be responsible for more variability in assemblage compositions than is presently acknowledged.

Distribution patterns of extant organic-walled dinoflagellate cysts (or dinocysts) in marine sediments are intensively studied throughout the world's oceans. Since the first comprehensive studies in the 1960s–1970s, knowledge on the ecological preferences of modern cyst-forming species steadily grew and today comprises information on species–environmental relations from various marine ecosystems (cf. Marret and Zonneveld 2003 and references therein). As a result, fossil archives are nowadays a well-established tool for palaeoenvironmental reconstructions, notably in neritic and sea ice settings (e.g., Mudie et al. 2001). The fact that dinocysts demonstrate high preservation potentials and sensitively reflect even small changes in temperature, salinity, and nutrient availability has greatly expanded the understanding of palaeoecological conditions (de Vernal et al. 2005; Pospelova et al. 2006). This source of information not only is complementary to other tracers but can be advantageous when calcareous and

siliceous microfossils suffer from dissolution. However, conclusions on (palaeo)environmental condition deduced from dinocyst assemblages in marine sediments also require information on the extent to which associations underwent changes after production. Dale (1996), for instance, considers the vast majority of dinocysts beyond the shelfbreak to have been transported there from neritic environments. Appreciation of taphonomic control is therefore important, not least because dinoflagellate biocoenoses react to the environment at an instant in time, whereas the thanatocoenosis usually reflect conditions of hundreds to thousands of years.

In efforts to communicate another factor of dinocyst taphonomy, some palynologists refer to the effect of dinocyst degradation as selective preservation and alert to the possibility of postdepositional skewing of associations due to oxidation (Hopkins and McCarthy 2002; Zonneveld et al. 2007). For good reason, the use of strong acids, acetolysis, and base treatment are avoided as much as possible during palynological processing because such procedures would destroy many peridinioid species, notably the brown-walled taxa (Hopkins and McCarthy 2002). As yet, only few studies qualitatively inferred this differential preservation of Quaternary cyst taxa from sediment cores (Zonneveld et al. 2001b; Versteegh and Zonneveld 2002; McCarthy et al. 2004; Zonneveld et al. 2007) so that the relevance in natural settings is still limited to speculations. This situation demands intensified research to assess the relation between groups of dinocysts and bottom-water oxygen contents.

¹ Corresponding author (frankd@rcom-bremen.de)

Acknowledgments

We thank the technical personnel of the research group Historical Geology/Palaeontology of Bremen University for their general support and all other members for their openness to discussion. We thank the anonymous reviewers for their constructive comments on the manuscript.

This research was carried out within the Research Center “Ocean Margins” (RCOM) at Bremen University (publication no. 0507) funded by the DFG (Deutsche Forschungsgemeinschaft).

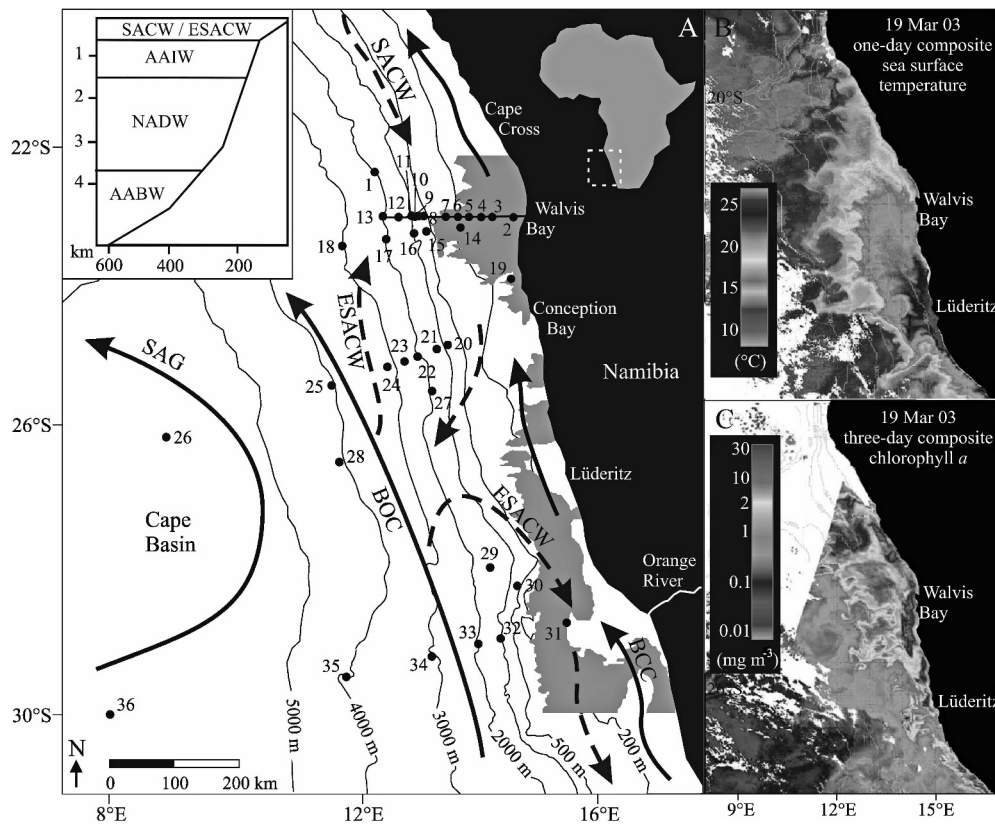


Fig. 1. (A) Map showing surface (solid arrows), subsurface currents (dashed arrows), and the principal water mass stratification in the Benguela upwelling region. BCC, Benguela Coastal Current; BOC, Benguela Oceanic Current; SAG, South Atlantic gyre; SACW, South Atlantic Central Water; ESACW, East SACW; AAIW, Antarctic Intermediate Water; NADW, North Atlantic Intermediate Water; AABW, Antarctic Bottom Water. Modified after Shannon and Nelson (1996). Area of annual mean bottom water oxygen content $<0.5 \text{ mL L}^{-1}$ as derived from model results (see below) is gray shaded. Location of 23°S transect shown in Fig. 2 is indicated. (B) One-day composite of sea surface temperature showing strongest upwelling of cold, thermocline water at latitude of Lüderitz. (C) One-day composite of chlorophyll *a* concentrations in surface waters showing highest pigment contents north of Lüderitz and filament induced offshore transport. Color images of B and C are available from Zabel et al. (2005).

Studies on dinocyst distribution patterns coming from areas with strong bottom-water oxygen gradients probably contribute most to a better understanding of taphonomic effects. We focused on the Benguela Current Upwelling System off Namibia (herein referred to as the BCUS), where hydrography and atmospheric conditions promote intense production, high particle flux rates, and, ultimately, severe bottom-water oxygen deficiencies ($\text{O}_2 < 2 \text{ mL L}^{-1}$) that locally give way to quasi-permanent oxygen minimum zones (Chapman and Shannon 1985). Although parameters commonly associated with dinocyst distribution are found as steep gradients, associations in surface sediments show patterns that are difficult to explain by differences in cyst production or lateral transport (e.g., Davey and Rogers 1975; Zonneveld et al. 2001a). To investigate whether the pattern in assemblage structure relates to the bottom-water oxygen regime, we raised species inventories of 36 surface sediment samples recovered from the continental shelf, slope, and rise as well as the abyssal Cape basin. The data were analyzed with respect to physical, chemical, and

biological factors applying multivariate techniques of ordination. On the scale of investigation, our approach attaches importance to the role of oxygen and alludes to consider marine palynomorphs as degradable organic particles in order to safeguard accurate interpretation of dinocyst associations.

Material and methods

Study area—The study area stretches along the Namibian coast between 22°S and 30°S and in its largest offshore extension reaches the Cape Basin at about 8°E, where water depths exceed 5,000 m (Fig. 1). Surface hydrography relates to the equatorward flow of the Benguela Current (Shannon and Nelson 1996). Shoreward, the flow of the Benguela Coastal Current and prevailing southeasterly winds drive upwelling of nutrient-rich water from depths between 200 and 300 m. This water can comprise different proportions of South Atlantic Central Water (SACW) and East SACW (ESACW). The former is bounded by the shelf

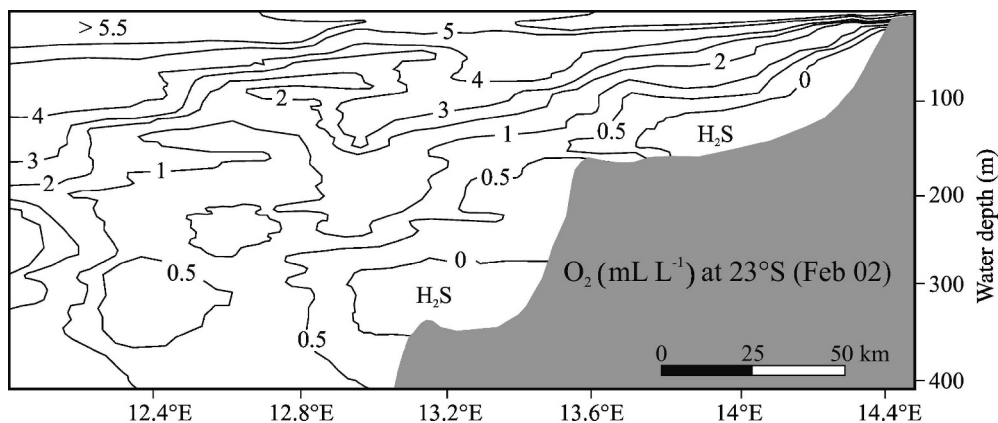


Fig. 2. Section of dissolved oxygen in the upper 400-m along 23°S (for location, see Fig. 1). In some areas, free H₂S can occur in the water column. A colored image is available from Zabel et al. (2005).

and travels south by a poleward undercurrent. Low oxygenation of SACW (<1 mL L⁻¹) and ongoing oxygen consumption during bacterial break down of organic matter promote the establishment of oxygen minimum zones over the shelf and upper slope at a depth between 100 and 450 m (Bailey 1991; cf. Fig. 2). Off the shelf, an increasing fraction of ESACW accounts for the northward advection of oxygen-rich but nutrient-depleted water from the Agulhas Retroflexion that is transported by the Benguela Oceanic Current. Cross-shelf circulation intensifies south of ~26.5°S, where well-ventilated ESACW becomes the dominant water mass limiting the southward extension of SACW to the latitude of Lüderitz. Below the thermocline, the flow of salty, less oxygenated Antarctic Intermediate Water (~3–4 mL L⁻¹) is similar to overlying waters. Beneath, a southward flowing stratum of high-saline, oxygenated North Atlantic Deep Water reaches down to depth of about 3,800 m and overlies Antarctic Bottom Water at abyssal depth (Shannon and Nelson 1996).

For much of the year, the strongest upwelling prevails in cells along the continental shelf, but Ekman transport in corridors of strong winds and the interaction of tides and topography may induce enhanced productivity above the shelf edge and upper slope (Lutjeharms and Meeuwis 1987). During austral summer and early autumn, the relaxation of wind stress and subsequent intrusion of warm, saline waters from the Angola Basin weaken the upwelling intensity. Usually, a thermal front at the shelf edge separates the cold, productive water from warm, subtropical water but recurrently is penetrated by eddies, filaments, and plums (Fig. 1). Nutrient concentrations of upwelled water can attain up to 20 μmol L⁻¹ of nitrate, 1.5 μmol L⁻¹ of phosphate, and 15–20 μmol L⁻¹ of silicate (Chapman and Shannon 1985). The average annual production north of the Orange River has been estimated to about 2 g C m⁻² d⁻¹ (Shannon et al. 1986), whereby chlorophyll *a* (Chl *a*) concentrations are lower during intense upwelling but increase during quiescent phases, when stratification recovers. They are also lower off Lüderitz (~27°S) but higher downstream of the cell (Bailey 1991). Diatoms bloom in the turbulent, nutrient-rich waters

of upwelling centers, while the phytoplankton community changes toward flagellate-dominated assemblages under stratified, nutrient-depleted conditions over the middle and outer shelf (Shannon and Pillar 1986).

The bottom topography is characteristic of an inner and outer shelf break at the 140- to 180-m and the 360- to 400-m contours, respectively. Except for few inner shelf areas, nannofossil and foraminiferal ooze constitute the bulk of sediments accumulating at high rates on the continental margin (Rogers and Bremner 1991). Among the biogenic deposits on the shelf, highest amounts of organic carbon (>15%) are recorded in a diatomaceous mud belt between 21°S and 25.5°S (Inthorn et al. 2006). A distinct depocenter with enhanced organic carbon loads (~9%) exists on the upper continental slope between 24°S and 26.5°S in water depths of 400 to 1,500 m. Terrigenous material supplied by perennial river discharge (Orange River) and aeolian dust from the Namibian Desert have little influence on the sediment texture (Shannon and Nelson 1996). Erosion and export of organic matter from the middle and outer shelf to the slope are provoked by cross-shelf circulation and lateral transport of particles in nepheloid layers (Inthorn et al. 2006). Because of the topography, we assume that slumps or slides do not represent significant transport processes.

Samples and processing—Dinocyst counts refer to 36 surface sediment samples, recovered during R/V *Meteor* cruises M20/2, M34/2, M34/1, M57/2, and M57/3 (Fig. 1; Table 1). The samples comprised the top centimeter of multi- and box cores and consisted mainly of diatomaceous mud or calcareous ooze with varying proportions of sand and clay. Because of areal changes in sedimentation rates (Mollenhauer et al. 2004), sediments are likely younger in nearshore settings and older in deep-sea regions, but information from oxygen isotope and AMS ¹⁴C-dated cores taken at or in the vicinity of the sample positions implies that all are late Holocene in age (cf. data sets doi:10.1594/PANGAEA.53229 and doi:10.1594/PANGAEA.71223 available online at the PANGAEA data archive, <http://www.pangaea.de>). Since climatic and oceanographic conditions during the late Holocene were relatively stable and

Table 1. Station list, basic lithology, and total dinocyst concentrations of analyzed samples.

No.	Event label	Cruise	Gear*	Latitude (°S)	Longitude (°E)	Depth (m)	Lithology	Total dinocysts (No. of g ⁻¹)
1	GeoB3608-1	M57/3	MUC	22°21.69	12°12.09	1,972	Foraminiferal-nannofossil ooze	9,250
2	184-3	M20/2	MUC	23°00.00	14°22.05	44	Diatomaceous ooze	49,438
3	187-3	M20/2	MUC	23°00.03	14°02.94	130	Diatomaceous ooze	77,993
4	188-3	M57/3	MUC	22°59.94	13°51.94	143	Diatomaceous ooze	46,120
5	212-3	M57/3	MUC	22°59.97	13°41.01	152	Diatomaceous ooze	8,997
6	213-3	M57/3	MUC	22°59.97	13°29.94	234	Clayey nannofossil ooze	11,995
7	191-5	M57/3	MUC	23°00.00	13°18.72	360	Clayey nannofossil ooze	11,663
8	173-2	M57/3	MUC	22°59.97	12°56.98	591	Clayey nannofossil ooze	15,895
9	GeoB8482-2	M57/3	MUC	22°59.97	12°53.52	706	Calcareous ooze	27,618
10	GeoB8483-1	M57/3	MUC	22°59.64	12°50.64	805	Foraminiferal-nannofossil ooze	15,489
11	GeoB8484-3	M20/2	BC	23°00.00	12°46.98	953	Calcareous ooze	14,926
12	GeoB8498-2	M20/2	MUC	23°00.03	12°34.95	1,439	Foraminiferal-nannofossil ooze	18,492
13	176-3	M20/2	BC	23°00.06	12°20.01	2,073	Calcareous ooze	6,586
14	GeoB1714-1	M20/2	BC	23°08.19	13°32.49	200	Clayey nannofossil ooze	10,809
15	GeoB1713-5	M20/2	BC	23°13.00	13°00.70	600	Clayey nannofossil ooze	21,131
16	GeoB1712-2	M20/2	BC	23°15.19	12°48.30	1,004	clayey foraminiferal-nannofossil ooze	37,095
17	GeoB1711-5	M20/2	BC	23°19.00	12°22.39	1,975	Foraminiferal-nannofossil ooze	16,932
18	GeoB1710-2	M20/2	BC	23°25.80	11°41.40	2,995	Foraminiferal-nannofossil ooze	3,699
19	GeoB3607-1	M20/2	BC	23°53.28	14°19.89	97	Diatomaceous ooze	172,800
20	GeoB3717-1	M20/2	BC	24°49.99	13°21.00	855	Clayey foraminiferal-nannofossil ooze	60,813
21	GeoB3718-8	M20/2	BC	24°53.70	13°09.69	1,313	Clayey foraminiferal-nannofossil ooze	20,833
22	GeoB3719-2	M20/2	MUC	24°59.70	12°52.29	1,995	Clayey nannofossil ooze	15,333
23	GeoB3720-1	M34/1	BC	25°04.08	12°40.08	2,516	Foraminiferal-nannofossil ooze	14,179
24	GeoB3721-4	M34/1	MUC	25°09.09	12°24.00	3,014	Clayey nannofossil ooze	14,340
25	GeoB3723-2	M34/1	MUC	25°23.70	11°31.59	4,004	Clayey foraminiferal-nannofossil ooze	6,377
26	GeoB3724-1	M34/2	MUC	26°08.29	8°55.60	4,766	Nannofossil ooze	4,063
27	GeoB3606-2	M34/2	MUC	25°27.99	13°04.98	1,793	Silicious nannofossil ooze	66,217
28	GeoB1715-1	M34/2	MUC	26°28.59	11°38.19	4,097	Foraminiferal-nannofossil ooze	6,480
29	GeoB1716-2	M34/2	MUC	27°57.10	14°00.19	1,485	Foraminiferal-nannofossil ooze	42,738
30	GeoB1717-2	M34/2	MUC	28°12.49	14°25.39	603	Sandy + clayey nannofossil ooze	5,121
31	GeoB1718-1	M34/2	MUC	28°42.49	15°12.60	167	Sandy + clayey diatomaceous ooze	4,645
32	GeoB1719-5	M34/2	MUC	28°55.60	14°10.39	1,023	Foraminiferal-nannofossil ooze	25,639
33	GeoB1720-4	M57/2	MUC	29°00.00	13°49.69	2,011	Foraminiferal-nannofossil ooze	8,675
34	GeoB1721-4	M57/2	MUC	29°10.50	13°05.29	3,079	Foraminiferal-nannofossil ooze	559
35	GeoB1722-3	M57/2	MUC	29°26.89	11°45.00	3,971	Nannofossil ooze	333
36	GeoB1724-4	M57/2	MUC	29°58.30	8°02.50	5,102	Clayey nannofossil ooze	1,139

* MUC, multicorer; BC, box corer/grab.

similar to those prevailing today (Grootes et al. 1993), samples are presumed to represent present-day dinocyst associations with an acceptable degree of accuracy.

Quantitative dinocysts analyses were conducted with approximately 1 cm³ of dried sediment (at 60°C overnight), which were dissolved in 10% hydrochloric acid to remove the carbonate content. Afterward, they have been washed thoroughly, decanted, and subsequently treated with cold 38% hydrofluoric acid to remove silicates. On 2 d of exposure, samples were neutralized with 40% potassium hydroxide. To avoid dinocyst dissolution, care was taken that the solution did not become alkaline at any time. The neutralization was necessary, as the nickel precision sieve (Stork Veco, mesh 570) with which the size fraction >20 μm was collected is not resistant to either acids or bases. The residue was centrifuged (3,500 rpm for 8 min), transferred into a 1.5-mL Eppendorf reaction vessel, and concentrated to 1 mL. An aliquot of the homogenized residue, depending on the amount of remaining material, was placed on a microscope slide, embedded in glycerin

jelly, and sealed with paraffin wax. At least one whole slide was counted for dinocyst species. Whenever a slide contained fewer than 200 dinocysts, an additional one was counted. A list of identified species and their relative abundance is provided in Web Appendix 1, Table A1.1 (http://www.aslo.org/lo/toc/vol_52/issue_6/2582a1.pdf).

Dinocysts have been termed according to their fossil names, as application of motile names was insufficient to differentiate them down to the species level. Generic groups designated with “spp.” include species of a similar genus that were not identifiable at the species level because of unsuitable orientation, adherence of debris, or the inability to spot typical taxonomic features. The group *Brigantedinium* spp. comprises all spherical brown protoperidinioid cysts without processes. The taxonomy used for this study is in accordance with Williams et al. (1998). Species of the genus *Echinidinium* have been described in Zonneveld (1997).

Environmental data—The environmental parameters selected for the multivariate analyses of dinocyst distribu-

tion in the BCUS cover a wide range of potentially important gradients. Annual mean bottom-water oxygen concentrations (adO₂) were derived from model results gained with a regional implementation of the Modular Ocean Model-31 (MOM-31; Geophysical Fluid Dynamics Laboratory, NOAA Department of Commerce, Princeton, NJ; <http://www.gfdl.noaa.gov>). Theory and concept of MOM-31 are explained elsewhere (Pacanowski and Griffies 1999). The circulation model is coupled with an ecosystem model as described in Fennel and Neumann (2004). Oxygen sources are photosynthesis and exchange with the atmosphere, while consumption is due to respiration and bacterial mineralization of detritus in the sediment and water column. Lateral ventilation by the Ekman compensation current and by the poleward undercurrent plays an important role in maintaining the permanent oxygen deficit of the shelf water. The horizontal model resolution in the area of investigation is about 8 km and compares with the cross-shelf station distance. Simulations were run over five model years for 1999–2005. The calculated adO₂ values used in this study correspond to 2003, as this year represented the most consistent data set.

Total organic carbon (TOC) contents of surface sediments were gathered from the PANGAEA archive (doi:10.1594/PANGAEA.53229, doi:10.1594/PANGAEA.71218, and doi:10.1594/PANGAEA.71223, available online at <http://www.pangaea.de>) and from literature records (Rogers 1977; Bremner 1981; Calvert and Price 1983). In total, data include 602 locations, of which 83% are from stations above 1,000-m water depth, resulting in a higher data density for the shelf and upper slope. Average summer and winter sea surface temperature (SSST, WSST) and salinity (SSSS, WSSS) values, as well as annual mean sea surface concentrations of phosphate (aPO₄) and nitrate (aNO₃), were derived from the World Ocean Atlas 2001 Data Set (National Oceanographic Data Center, Silver Springs, MD; <http://www.nodc.noaa.gov/OC5>). Upper water column stratification during summer (SSI) and winter (WSI) was indicated by the Brunt-Väisälä frequency ($N = \sqrt{[9.8\delta D]/[1.026\delta z]}$), where δD represents the density difference calculated with the standard NICMM equation (Pond and Pickard 1983) for temperature and salinity change over δz (in this case 50 m). Seasonal concentrations of Chl *a* (SChl *a*, WChl *a*) for 2001 have been inferred from ocean color scan images that are available by the SeaWiFS Project (NASA Goddard Space Flight Center, Greenbelt, MD; <http://oceancolor.gsfc.nasa.gov/SeaWiFS>) at a grid size of ¼ degree. In all cases, seasonality refers to northern hemisphere summer (Jul–Sep) and winter (Jan–Mar).

To finally determine a value at each of the 36 sample locations, all environmental variables have been interpolated horizontally with inverse distance weighting, a mapping method build in Surfer v8 (Golden Software, Inc.). Depth was not considered separately within the statistical analyses because its relationship to species distribution is clearly coincidental with any dependence of other variables on depth. Data and descriptive statistic of the environmental variables used for multivariate analyses are given in Web Appendix 1, Table A1.2.

Table 2. List of species included in statistical analysis, their nutrition, and taxonomic classification.

Species/taxon	Abbr.	Order* (trophy†)
<i>Bitectatodinium tepikiense</i>	<i>Btep</i>	G (a)
<i>Echinidinium aculeatum</i>	<i>Eacu</i>	P (h)
<i>Echinidinium delicatum</i>	<i>Edel</i>	P (h)
<i>Echinidinium granulatum</i>	<i>Egra</i>	P (h)
<i>Echinidinium</i> spp.	<i>Espp</i>	P (h)
<i>Echinidinium transparentum</i>	<i>Etra</i>	P (h)
<i>Impagidinium aculeatum</i>	<i>Iacu</i>	G (a)
<i>Impagidinium paradoxum</i>	<i>Ipar</i>	G (a)
<i>Impagidinium patulum</i>	<i>Ipat</i>	G (a)
<i>Impagidinium plicatum</i>	<i>Ipli</i>	G (a)
<i>Impagidinium sphaericum</i>	<i>Isph</i>	G (a)
<i>Impagidinium striatum</i>	<i>Istr</i>	G (a)
<i>Impagidinium variaseptum</i>	<i>Ivar</i>	G (a)
<i>Nematosphaeropsis labyrinthus</i>	<i>Nlab</i>	G (a)
Cyst of <i>Protoceratium reticulatum</i>	<i>Pret</i>	G (a)
<i>Operculodinium israelianum</i>	<i>Oisr</i>	G (a)
Cyst of <i>Protoperidinium americanum</i>	<i>Pame</i>	P (h)
<i>Multispinula quanta</i>	<i>Mqua</i>	P (h)
Cyst of <i>Pentapharsodinium dalei</i>	<i>Pdal</i>	P (a)
<i>Polykrikos kofoidii</i>	<i>Pkof</i>	Gy (h)
<i>Trinovantedinium capitatum</i>	<i>Tcap</i>	P (h)
<i>Pyxidinospis reticulata</i>	<i>Pyxr</i>	G (a)
<i>Brigantedinium</i> spp.	<i>Bspp</i>	P (h)
<i>Selenopemphix nephroides</i>	<i>Snep</i>	P (h)
<i>Spiniferites mirabilis</i>	<i>Smir</i>	G (a)
<i>Spiniferites patchydermus</i>	<i>Spat</i>	G (a)
<i>Spiniferites ramosus</i>	<i>Sram</i>	G (a)
<i>Spiniferites</i> spp.	<i>Sspp</i>	G (a)

* G = Gonyaulacales; P = Peridinales; Gy = Gymnodinales.

† a, autotroph; h, heterotroph.

Statistical analysis—Eleven dinocyst species were removed from the original data set because they occurred only in three or fewer samples. These include *Dallella chathamensis*, *Gymnodinium catenatum*, *Lingulodinium machaerophorum*, *Pyxidinospis psilatatum*, *Polykrikos schwarzii*, *Polysphaeridium zoharyi*, *Spiniferites bulloides*, *Tectatodinium pellitum*, *Votadinium spinosum*, *Votadinium calvum*, and *Quinquecuspis concreta*. The remaining 28 species accounted for at least 94% of the total assemblage at each station and have been retained for statistical analyses (Table 2). Relative frequencies were used instead of concentrations per gram of sediment. This gave more weight to dominant species and potentially underestimated trends of less abundant cysts (“closed-sum effect”). Absolute numbers, however, were inappropriate for statistical analysis because of the extreme ranges in the data set, a disproportional weighting of rare cysts, and the effect of dilution by varying sedimentation rates.

A cluster analysis (Euclidean distances) based on the Jaccard (Ružička) index was conducted to identify provinces of similar assemblage structure, while species common to a province, in the sense that they appear at consistent (high) percentages in the corresponding samples, were inferred from SIMPER-analysis (similarity percentage). In order to point out relationships to latent environmental gradients, data were processed with detrended correspondence analysis (DCA; detrending by

second-order polynomial). This method demands species data only (indirect), but interpretation was facilitated by including the available environmental information. Subsequent to DCA, constrained (or canonical) correspondence analysis (CCA) was applied. This technique accounts for variability that can be explained “best” by the measured environmental parameters (direct). Therefore, variables had to be standardized to mean 0 and variance 1 in order to make them comparable. In CCA it is very popular to use all available parameters simultaneously. This, however, coevally relaxes constraining if the number of variables is high so that the results become similar to unconstrained ordination. Hence, CCA modeling has been accomplished to limit the number of variables to the most important ones. This was done by single-term addition (forward selection) of variables that met the Akaike Information Criterion goodness-of-fit criterion. Each selection was assessed by evaluating its contribution in terms of total deviance explained. Thereby, variables had to be significant at $p < 0.05$ of a chi-square test. As strong correlations exist among the candidate predictors, variance inflation factors (VIFs) were consulted as a measure of redundancy. The results obtained from ordination were finally cross-checked, consulting discriminant analysis in order to determine the degree of consistency between the final model and cluster analysis. For detailed background information on the statistical techniques mentioned here, we refer to more sophisticated literature (e.g., Legendre and Legendre 1998). All computations were done with R (Version 2.2.0), a programming environment for data analysis and graphics (<http://www.r-project.org>).

Results

After removing rare species from the data set, species richness corresponded to 13–24 taxa per sample, assuming that counting more than 200 specimens per sample eliminated further diversity. The total concentration of dinocysts per gram of sediment varied largely among sites (cf. Table 1) but generally declined between coastal and open ocean as well as northern and southern stations. The latter tendency was less pronounced.

Cluster analysis identified five groups of stations at a dissimilarity cutoff level of 70%, which we assigned to oceanic provinces (A–E in Fig. 3). Province A comprised epeiric sites above 250 m, located within the oxygen minimum zone off Walvis Bay. Province B ran parallel to the coast and merged most sites from the slope above 2,000 m and the sample from the Orange River mouth (31). Province C contained sites from the continental rise between 2,000 and 4,000 m north of $\sim 25.5^\circ\text{S}$ and province D mainly sites from a similar depth range but south of $\sim 25.5^\circ\text{S}$. Province E comprised the remaining three sites that located in the Cape Basin abyssal plain below 4,000 m. The relative contributions of single species to the similarity in each province were determined by SIMPER analysis (Table 3). Many species did not contribute to a large extent, and they were therefore not considered in great detail. Those with tendencies to dominate associations in the different provinces were *Brigantidium* spp., cyst of *P.*

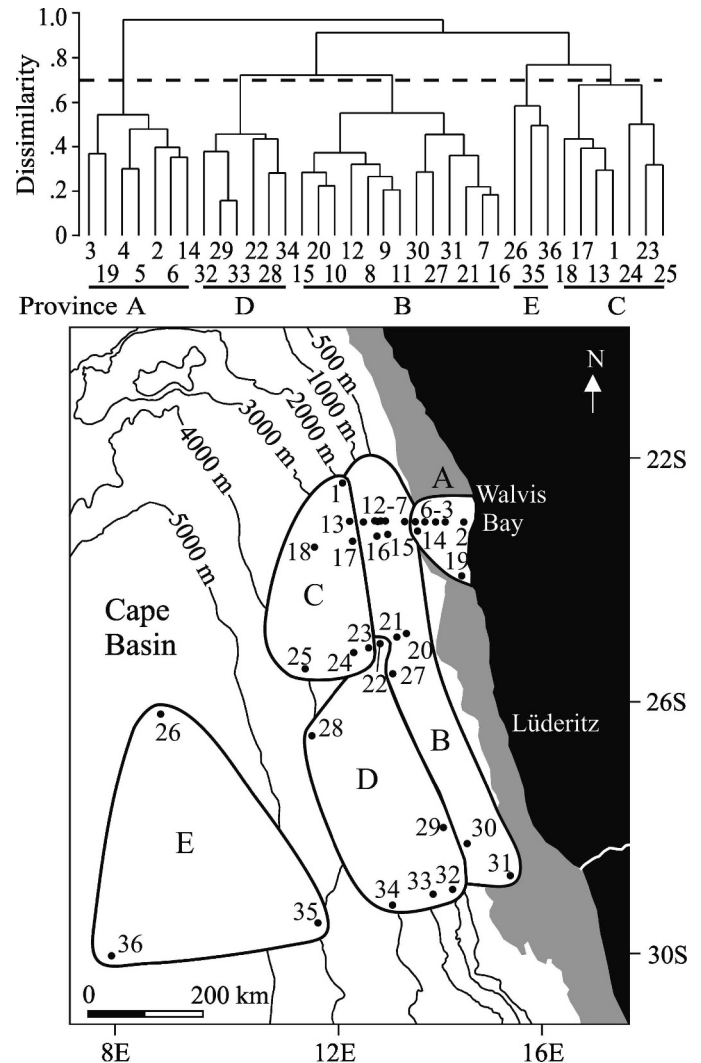


Fig. 3. (A) Results of cluster analysis. Dendrogram of species data showing groups of sample stations at the 70% dissimilarity cutoff level (dashed line). (B) The map indicates geographic locations of the identified provinces (A–E).

reticulatum, *N. labyrinthus*, and *I. aculeatum*. Generally, these species represented the good discriminators between provinces. Most conspicuous trends were observed for cysts of heterotrophic dinoflagellates, which accounted for $\sim 81\%$ similarity in province A. In provinces B and C, they declined considerably and were largely displaced by the cyst of *P. reticulatum* and *N. labyrinthus*, respectively. In province D, the relative abundance of cysts of heterotrophic dinoflagellates did not exceed 10% and became insignificant in province E, where *I. aculeatum* contributed most.

Graphical presentation of the DCA results allowed for the discrimination of the same provinces that had been identified by cluster analysis (Fig. 4). The first axis explained the largest part of the variation and represented a gradient (or combination of gradients) of proximal–distal (coastal–neritic–oceanic) change. The axis achieved maximal contrast between most shelfward stations bundled on the negative scale (province A) and samples from furthest

Table 3. Results of SIMPER-analysis.

Province	Species/taxon	Average abund. %	Average similarity	Contrib. %	Cum. %
A	<i>Bspp</i>	46.03	41.22	56.64	56.64
	<i>Espp</i>	12.26	8.93	12.27	68.91
	<i>Eacu</i>	6.43	4.55	6.25	75.16
	<i>Mqua</i>	6.39	4.21	5.79	80.95
	<i>Nlab</i>	6.42	3.89	5.35	86.29
	<i>Pret</i>	6.09	3.12	4.28	90.57
B	<i>Pret</i>	45.49	41.54	52.86	52.86
	<i>Bspp</i>	25.54	20.34	25.89	78.74
	<i>Espp</i>	6.23	4.60	5.85	84.60
C	<i>Nlab</i>	6.55	4.28	5.44	90.04
	<i>Nlab</i>	32.65	26.28	39.05	39.05
	<i>Pret</i>	18.41	13.99	20.79	59.84
	<i>Bspp</i>	18.74	12.11	17.99	77.83
	<i>Ipar</i>	3.38	2.43	3.62	81.45
	<i>Pyxr</i>	3.55	2.11	3.14	84.59
	<i>Iacu</i>	3.41	2.07	3.08	87.67
	<i>Espp</i>	4.35	2.02	3.00	90.68
	D	<i>Pret</i>	56.02	49.19	64.09
<i>Nlab</i>		12.88	9.24	12.04	76.13
<i>Bspp</i>		10.25	6.93	9.02	85.15
<i>Sram</i>		7.59	5.70	7.43	92.58
E	<i>Iacu</i>	26.90	19.34	30.11	30.11
	<i>Nlab</i>	17.10	15.05	23.43	53.54
	<i>Ipar</i>	9.32	8.54	13.30	66.84
	<i>Pret</i>	17.71	8.15	12.69	79.53
	<i>Pyxr</i>	2.73	2.14	3.34	82.87
	<i>Isph</i>	3.71	2.00	3.12	85.99
	<i>Sram</i>	2.84	1.80	2.80	88.79
	<i>Sspp</i>	3.21	1.75	2.73	91.52

offshore on the positive extreme (province E). The second DCA axis accounted for a smaller part of the variation and separated stations of provinces A and C on the positive scale from samples corresponding to provinces B, D, and E

on the negative part. The distribution of species scores illustrated affinities with respect to the underlying gradient(s). Opposed to the first DCA axis, most cysts of the heterotrophic genera plotted on the shelfward scale, while

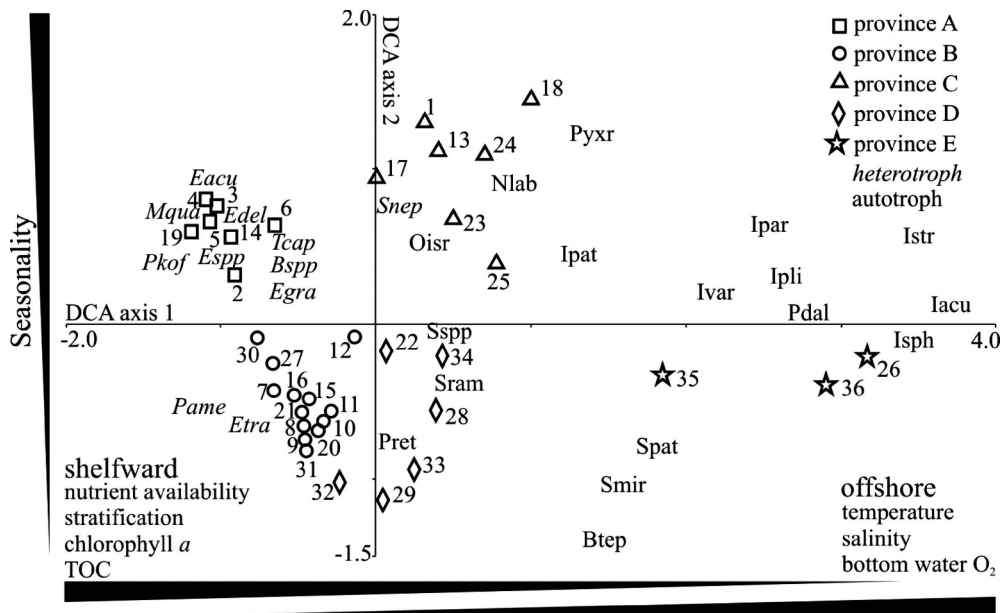


Fig. 4. DCA plot showing the variation between samples and variability in species distribution. Axes lengths are expressed in unit standard deviation. Relationships between sample scores and the environmental parameters are indicated by filled triangles.

Table 4. DCA summary and interset correlations (R^2) of environmental variables with axes scores. Estimates in bold are significant at $p < 0.05$.

	DCA1	DCA2	DCA3	DCA4
Eigenvalue	0.385	0.166	0.067	0.041
Cum. % of var.	36.4	52.2	58.5	62.4
adO ₂	0.707	0.104	0.061	-0.058
TOC	-0.662	0.119	-0.042	0.035
aPO ₄	-0.835	0.323	-0.048	0.014
aNO ₃	-0.860	0.237	-0.023	0.061
SSST	0.865	-0.081	0.107	0.062
WSST	0.837	-0.143	-0.010	0.037
SSSS	0.856	-0.117	-0.205	-0.057
WSSS	0.911	-0.156	-0.179	-0.040
SChl <i>a</i>	-0.628	0.256	-0.102	-0.064
WChl <i>a</i>	-0.467	0.329	0.081	-0.170
SSI	-0.812	0.234	0.012	0.151
WSI	-0.702	0.219	0.111	0.170

the cysts of autotrophic gonyaulacoids were distributed on the neritic-to-oceanic intercept. Most of the dinocysts that scored toward the extremes of DCA axis 2 were associated with a cosmopolitan distribution. The environmental predictors correlated significantly ($p < 0.05$) but differently strong with the site scores of the first DCA axis (Table 4). In the case of WSSS, this correlation explained 91% of the association captured by ordination but only about 70% in the case of adO₂. The second DCA axis proved a weak but significant relationship to WChl *a* (~33%).

From the available quantity of variables, the parameter combination best explaining community variability was determined by stepwise CCA modeling building. Forward selection identified a model composed of three sea surface parameters (WSSS, WChl *a*, and aPO₄) and adO₂ as a taphonomic factor (Table 5). The linear combination of these parameters and their direct relation to the variations in dinocyst assemblage composition were statistically significant (Monte Carlo permutation test: $p < 0.005$). The VIF of the variables did not exceed the critical value of 10 so that each addition accounted for independent information (i.e., covariance was negligible). This became apparent when their values were plotted against the site scores of the first CCA axis (Fig. 5). Vectors of WSSS and aPO₄ ran opposite one another and were linearly correlated to the first axis. In contrast, WChl *a* and adO₂ revealed a significant connection

with variability on the first axis by means of exponential and logistic coherence, respectively. The relationship between community variability and the conditionally significant parameters (i.e., covariance eliminated) has been summarized in Table 6. Constraining rendered only a part of the environmental ties, but in most cases at least one parameter explained a significant proportion of species variability. A major influence on ordination could be ascribed to species that accounted for the main differences between the provinces. Although these species obtained highest weights in CCA, model building carried out without them resulted in the same solution. After combining evidence inferred from regressions and correlations between species abundance and the determined predictors, five categories of dinocysts were recognized (note that the relationships always refer to the mean of a variable): (1) Species whose relative abundance showed a strong connection to increasing salinity values. This concerns *Impagidinium* species (except for *I. variaseptum*). (2) Species whose distribution showed a strong relationship to Chl *a* concentration in surface waters. Positive relationships were determined for *Brigantedinium* spp., *M. quanta*, *Echinidinium* spp., *E. aculeatum*, and *P. kofoidii*. Relationships were negative in case of *I. aculeatum*, *I. sphaericum*, and *S. mirabilis*. (3) Species whose relative abundance showed changes in the course of varying bottom-water oxygen concentrations. Inverse correlations were observed for cysts of *E. transparentum*, *T. capitatum*, cyst of *P. americanum*, and *M. quanta*. Positive relationships were determined for *P. reticulata*, *N. labyrinthus*, *S. ramosus*, and *I. patulum*. (4) Species whose contributions to the assemblage showed dependency on phosphate concentrations in surface waters. Positive relationships were shown by cysts of *Brigantedinium* spp., *Echinidinium* spp., *E. delicatum*, and *E. granulatum*. Negative relationships were assessed for *N. labyrinthus*, *P. reticulata*, *S. ramosus*, *S. mirabilis*, and *B. tepikiense*. (5) Species whose distribution pattern showed little or no relation to any of the given variables (i.e., cyst of *P. reticulatum*, *O. israelianum*, *P. dalei*, *I. variaseptum*, *S. patchydermus*, *Spiniferites* spp., and *S. nephroides*).

The results of discriminant analysis are shown in Table 7. The use of WSSS, WChl *a*, adO₂, and aPO₄ as explanatory variables was highly significant (Wilks's lambda = 0.051, df = 12, $p < 0.001$) and accounted for a total of 81% correctly predicted classifications. Two stations of province A (6, 14) were incorrectly assigned to province B, three stations (12, 21, 25) of province B were

Table 5. Description and results of stepwise CCA model building.

	CCA1	CCA2	CCA3	CCA4	df	AIC*	Deviance	Residual deviance	% of dev. explained	Pr (χ^2)†	VIF‡
Eigenvalues	0.333	0.125	0.067	0.038							
Cum % var.	31.5	43.4	49.7	53.3							
None					—	169.64	3,790.54	—	—	—	—
WSSS					-1	158.26	1,177.07	2,613.47	31.1%	0.00025	7.43
WSSS + WChl <i>a</i>					-2	154.70	373.91	2,239.56	40.9%	0.01839	1.57
WSSS + WChl <i>a</i> + adO ₂					-3	152.52	245.22	1,994.34	47.4%	0.04103	2.14
WSSS + WChl <i>a</i> + adO ₂ + aPO ₄					-4	150.15	228.07	1,766.27	53.4%	0.03654	7.12

* Akaike Information Criterion.

† Refers to the addition of the variable.

‡ Value of added variable in the final model.

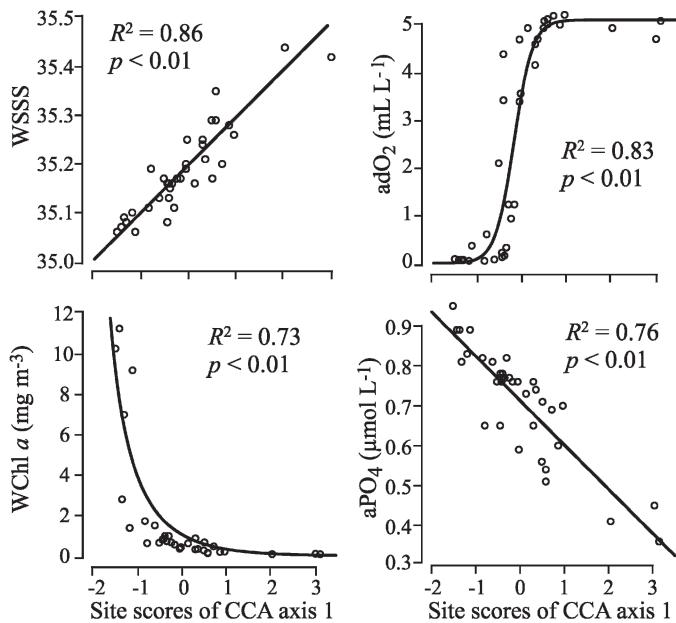


Fig. 5. Regressions between site scores of the first CCA axis and the environmental parameter included in the final CCA model. Different trend lines have been fitted to the data: WSSS and aPO_4 = linear, WChl a = exponential, adO_2 = logistic.

grouped in province C, and two stations (22, 27) were confused between provinces C and D. Stations of province E were classified correctly throughout. Classifications that did not correspond to the results of cluster analysis were in most cases attached to stations from the upper slope.

Discussion

Cyst production—Heterotrophic dinoflagellates, notably the genus *Protoperidinium*, are typically thought to be abundant in high productivity regimes, whereas increasing cyst formation by autotrophic species is often considered to indicate the transition to predictable and nutrient-poor conditions (Wall et al. 1977; Harland et al. 1998; Radi and de Vernal 2004). Our results show that cysts of heterotrophic dinoflagellates dominate the assemblage close to coastal upwelling, whereas cysts of autotrophic species dominate in neritic to oceanic environments (cf. Table 3). One could think of this analogy as a basic explanation for dinocyst community variability in the BCUS. However, recent studies show that cysts of several autotrophic dinoflagellates can be more abundant in areas of increased nutrient availability and high productivity in surface waters as compared to oligotrophic regions (Susek and Zonneveld 2005; Radi et al. 2007; Zonneveld et al. 2007). Accordingly,

Table 6. Simplified relationships between species and results of CCA. Multiple linear regressions between species distribution and the CCA model and rank correlations between environmental variables and species.

Species/taxon	CCA weight	Adj. R^2 model*	†			
			WSSS	WChl a	adO_2	aPO_4
<i>Edel</i>	14.61	*0.262	–	+	–	(+)
<i>Egra</i>	52.30	0.234	–	+	–	(+)
<i>Bspp</i>	854.79	*0.609	–	(+)	–	(+)
<i>Espp</i>	210.01	*0.568	–	(+)	–	(+)
<i>Eacu</i>	72.04	*0.678	–	(+)	–	+
<i>Pkof</i>	6.86	*0.281	–	(+)	–	+
<i>Mqua</i>	74.26	*0.349	–	(+)	(–)	+
<i>Pame</i>	31.96	*0.564	–	+	(–)	+
<i>Tcap</i>	68.02	0.157	–	+	(–)	+
<i>Etra</i>	26.57	*0.299	–	+	(–)	+
<i>Snep</i>	34.37	0.242				
<i>Oisr</i>	8.32	0.004				
<i>Sspp</i>	46.28	0.207				
<i>Pret</i>	1,152.06	*0.283		(–)		
<i>Pdal</i>	11.89	0.203	(–)			
<i>Spat</i>	5.69	0.225	(–)			
<i>Ivar</i>	14.10	*0.372	(–)			(–)
<i>Ipat</i>	14.78	*0.262	(+)	–	(+)	–
<i>Ipli</i>	3.78	*0.421	(+)	–	+	–
<i>Ipar</i>	61.29	*0.657	(+)	–	+	–
<i>Istr</i>	8.76	*0.473	(+)	–	+	–
<i>Isph</i>	15.70	*0.624	(+)	(–)	+	–
<i>Iacu</i>	115.88	*0.604	(+)	(–)	+	–
<i>Smir</i>	17.09	*0.624	+	(–)	+	(–)
<i>Btep</i>	2.89	0.157	+	–		(–)
<i>Sram</i>	128.92	*0.629	(–)		(+)	(–)
<i>Nlab</i>	487.24	*0.485	+	–	(+)	(–)
<i>Pyxr</i>	45.42	*0.449	+	–	(+)	(–)

* Significant ($p < 0.01$) multiple regressions have an asterisk.

† Spearman rank correlation: +/- = positive/negative ($p < 0.05$); otherwise, insignificant. Parentheses indicate parameter explaining significant proportion of species variability ($p < 0.05$).

Table 7. Jackknifed matrix of discriminant analysis showing the classification of sample stations by the final CCA model (cases in row categories classified into columns).

Province	A	B	C	D	E	% correct
A	5	2	0	0	0	71
B	0	10	3	0	0	77
C	0	0	6	1	0	86
D	0	0	1	5	0	83
E	0	0	0	0	3	100
Total	5	12	10	6	3	81

prevalence of peridinioid cysts close to the upwelling domain is not necessarily synonym to autotrophic dinoflagellates being systematically displaced by heterotrophic species. Using relative abundance data for our approach could have amplified this tendency accentuating the dominance of peridinioids, which may outnumber autotrophic species in terms of frequency and efficiency of cyst formation. Further studies on this issue will therefore need to consider autecological aspects, keeping in mind that life-form selection and development of dinoflagellate blooms with subsequent encystment may strongly depend on seasonal changes in hydrography and wind trajectories in nearshore zones of the BCUS (Pitcher et al. 1998; Pitcher and Nelson 2006).

Transport—Studies on particle flux, carbon turnover, and sedimentation processes point to the relevance of lateral transport in the BCUS (Inthorn et al. 2006). Accordingly, shelf break and upper slope may receive cyst input from the outer shelf because of transport in the benthic and intermediate nepheloid layers. This process could explain the deviant grouping of some stations from the upper slope, as is observed by cluster analysis and discriminant analysis (Table 7). On the shelf, dinoflagellates are probably also displaced from the upwelling center by the equatorward current, but cyst flux into the poleward undercurrent may prevent washout from the inner shelf. Such a recirculating loop is described for diatoms in an upwelling area off southwestern Africa (Pitcher 1990). The major consequence for cyst transport is that the bulk of cysts produced over the inner and middle shelf are most likely not transferred to outer domains but accumulate in the mud belt north of Lüderitz and below the Walvis Bay upwelling cell. In these high productivity zones, mechanisms such as agglomeration and flocculation in “marine snow” (Lampitt et al. 1993) and transport in fecal pellets (Mudie 1996) may further accelerate the export of cysts to bottom sediments, thereby reducing the time span for transportation.

Most cysts behave like silt particles and could cover long distances from their point of formation to the site of sedimentation by both surface water and deep-water transport (Dale 1996). We found high contributions of cysts of *P. reticulatum* and *S. ramosus*, both prominent to the Agulhas Current region and the southwestern shelf of Africa, respectively (Davey and Rogers 1975). Transport associated with the Benguela Current could have supplied these species to the BCUS, notably to stations influenced by ESACW (cf. Fig. 1). On the other hand, Zonneveld et al. (2001a)

concluded that cyst input from different remote sources has marginal influence on assemblages in the BCUS. A predominantly autochthonous character of the association is also inferred from our database that only sporadically includes species typical for the Atlantic sector of the Southern Ocean, the southern Indian Ocean, and the Angola Basin (Marret and Zonneveld 2003 and references therein).

Environmental control: Sea surface conditions—According to our results, community variability explained by CCA modeling strongly relates to WSSS, which influences the distribution of *Impagidinium* species, *P. dalei*, *S. ramosus*, and *S. patchydermus* (Table 6). This is in contrast to findings of Zonneveld et al. (2001a), who identified a strong stratification signal in their study of the Benguela region. However, their sampling covered more stations near to Orange River outflow, where the stratification gradient was probably steepest. In our study area, salinity differences are greatest between active upwelling centers and the open-ocean domain and may therefore exert a stronger influence than water column stability. Species that are inversely related to WSSS comprise exclusively heterotrophic taxa, which could be indicative of their prevalence in the vicinity of high-productivity centers where low-saline waters are upwelled from the subsurface.

The Chl *a* concentration, in particular, is an indicator for primary production, and in our study WChl *a* is positively related to the distribution of some peridinioid species (Table 6), suggesting an indirect relationship to phytoplankton growth. The encystment may attain highest rates after phytoplankton blooms have established in austral summer in response to weaker upwelling. Some species are negatively related to WChl *a*. All are produced by autotrophic dinoflagellates and described predominantly from oligotrophic habitats that accord to their light requirements (Marret and Zonneveld 2003). The link between WChl *a* and community variability may further cover a seasonal component, as is indicated by DCA (Table 4; Fig. 4). The second axis opposes cysts of heterotrophic dinoflagellates that are adapted to seasonal cues (Edwards 1993) and most *Spiniferites* species, which prefer areas of little seasonal contrast (Vink et al. 2000). The former are abundant in areas of strong seasonal changes in Chl *a* concentration (i.e., near to upwelling cells and in the filament sector), while the latter tend to higher contributions in more predictable provinces.

Nutrient concentrations in surface waters exert strong control on the distribution of dinocysts (Marret and Zonneveld 2003). CCA model building has selected the annual phosphate concentration, which shows a positive relation with cysts of *Brigantedinium* spp. and most *Echinidinium* species. In modern sediments, vast numbers of the former are found in areas of elevated nutrient contents (Rochon et al. 1999), but they are also prominent in habitats with periodical nutrient enrichment (McMinn 1992). In the eastern South Atlantic, cysts of the genus *Echinidinium* are observed in the vicinity of upwelling of fertile waters (Zonneveld et al. 2001a) and in the western equatorial Atlantic in association with high nutrient input from river discharge (Vink et al. 2000). Species with

negative relations to phosphate, in particular of the genera *Impagidinium* and *Nematosphaeropsis*, are often related to rather nutrient-poor environments (Wall et al. 1977). This agrees with the association in province E, but our results suggest that they can also prosper in areas where filament activity causes episodic nutrient delivery so that high relative abundances do not necessarily mirror an oligotrophic open-ocean environment. Interestingly, many studies infer a stronger nitrogen control on dinoflagellates (e.g., Devillers and de Vernal 2000). In the BCUS, nitrogen is the limiting component, but phosphate may become more important during the growth season, as it is less homogeneously distributed (i.e., stronger gradient).

Taphonomic control: The role of oxygen—For terrestrial palynomorphs, differential susceptibility to oxidation is evident from the study of Quaternary pollen (Campbell 1999). By comparison to terrestrial compounds, Versteegh and Zonneveld (2002) hypothesized that gonyaulacoid and peridinioid cysts represent end members in a degradability “ranking.” They expected significant shifts in assemblage compositions toward the former once the availability of oxygen in bottom and pore waters increases. Their theory agrees well with the result of SIMPER analysis (Table 3) and corresponds to the discrimination of heterotrophic peridinioids and autotrophic gonyaulacoids along the first DCA axis (Fig. 4). The low scattering of peridinioid cysts relative to stations of province A suggests that their sedimentary distribution particularly relates to strong oxygen deficiency. Similar conclusions have been drawn from a recent compilation of surface sediment accumulation data that shows that sensitive cysts are typically more abundant in oxygen-deficient zones compared to well-oxygenated sediments (Zonneveld et al. 2007).

McCarthy et al. (2003) argued that the common observation of an offshore increase in the gonyaulacoid: peridinioid ratio may result primarily from destruction of peridinioid cysts under oxidizing conditions rather than reflecting the true distribution of dinoflagellates in surface waters. In our study, the pattern emerging from community variability roughly depicts the local hydrography and ground-level oxygenation off Namibia as is described in Chapman and Shannon (1985) and Bailey (1991). Moreover, the results of CCA emphasize that the distribution of certain peridinioid taxa may particularly relate to this factor (Table 6). This is corroborated by laboratory experiments that reveal the different degradation behaviors of marine palynomorphs (Hopkins and McCarthy 2002). Moreover, reports on postdepositional organic matter degradation in natural settings indicate that the resistance of dinocysts to oxidation parallels their susceptibility to chemical treatment (Zonneveld et al. 2001b). According to these observations, species have been classified in ascending order of resistance as (1) highly sensitive (cysts formed by genus *Protoperidinium* and *Echinidinium*), (2) moderately sensitive (e.g., cyst of *P. reticulatum* and *Spiniferites* species), and (3) resistant (e.g., *Impagidinium* species, *N. labyrinthus*, and *O. israelianum*). An analogy to the present study exists in case of the sensitive categorization, but it is vague with respect to moderately sensitive and resistant dinocysts. However, the

positive relationship between oxygenation of bottom water and some gonyaulacoid species may indicate that their spatial variability is particularly governed by selective degradation of sensitive cysts.

The dependency between dinocyst distribution and adO_2 may be more appropriately described by a host of processes that characteristically prevail under conditions where oxygen is present. Accordingly, degradation/preservation could relate predominantly to the oxygen exposure time, as has been pointed out for fluxes of lipid biomarkers to surface sediments in the eastern South Atlantic (Schefuß et al. 2004). Apparently, it is difficult to account for all factors influencing the oxygen exposure time, such as sedimentation rates, resuspension, bioturbation, export production and amounts, and states and reactivity of compounds available for oxidation. We assume that most of these factors covary with bottom-water oxygen and would have a minor influence on our results if the oxygen exposure time were corrected for. However, we have to consider that the preservation of assemblages reaching the sediment-water interface may be partly or entirely independent of dissolved oxygen levels at high rates of sedimentation (Tyson 2001). In this case, bottom waters could be ventilated while pore waters may not because of rapid burial and enhanced oxygen consumption by bacteria. However, in situ pore-water measurements suggest that oxygen penetrates at least the very surface of the sediment at different sites (Glud et al. 1994; Zabel et al. 2005) so that high export fluxes do not categorically offset the use of overlying bottom-water oxygen concentrations.

Despite the use of modeled oxygen data, the paucity of samples at our disposal, and the uncertain time frames involved, we conclude that selective degradation, to some degree, has altered the initial pattern in species associations after cysts were buried to surface sediments, and in consideration of the factors discussed here, we describe the thanatocoenosis in bottom sediments of the BCUS as reflecting five domains: (1) The upwelling zone. This domain concerns the eutrophic, inner shelf area off Walvis Bay, where an oxygen minimum zone is developed for most of the year. Well-preserved, highest amounts of sensitive cysts produced by opportunistic species (i.e., of the genera *Protoperidinium* and *Echinidinium*) reflect high nutrient and pigment concentrations derived from intense but seasonal upwelling. Transport occurs downstream of the upwelling cell but is of minor importance in terms of community variability. (2) The transport realm. Including the shelf break front, this belt stretches parallel to the coastline covering the outer shelf and upper slope, where lateral transport in nepheloid layers and resuspension by bottom currents are of particular importance. An association typically dominated by the cyst of *P. reticulatum* relates to cyst production in matured waters. Although high contributions of *Brigantedinium* spp. can be observed, varying oxygenation of bottom waters and local changes in sedimentation rates probably provoke spatial heterogeneity in preservation of sensitive species. (3) The seasonal domain. Located in the pathway of major filament activity, this area over the continental rise receives periodical nutrient delivery in dependence on seasonal changes in

meridional wind stress. Higher abundances of *N. labyrinthus* compared to cysts of *P. reticulatum* or *Spiniferites* species are probably the result of a better adaptation to a relatively unstable environment. *Brigantedinium* spp. take advantage of the fertile waters associated with filament formation, and cyst production is sufficient to enable relatively high deposition despite permanent oxidation stress. (4) The Benguela Current domain. South of 25.5°S, conditions become more stable in terms of seasonality, while hydrography relates to a stronger influence of ESACW. The dinocyst association is characterized by highest contributions of cysts of *P. reticulatum* and the characteristic appearance of *S. ramosus*, both possibly also transported to the north along the advection path of the Benguela Oceanic Current. Conditions for the preservation of sensitive cysts deteriorate because of sufficient oxygenation of bottom waters so that the abundance of *Brigantedinium* spp. in the sediments does not necessarily reflect production in overlying waters. (5) The open-ocean realm. Furthest offshore, toward the oligotrophic waters of the South Atlantic gyre, conditions are favorable for photosynthesis. Cyst production in surface waters is likely low, and the typical representatives of the dinocyst association in sediments at abyssal depth are almost exclusively gonyaulacoids. Species of the genus *Impagidinium* become more important, but the extremely slow sedimentation rates and conditions favorable for selective degradation do not allow for a direct comparison to the plankton assemblage.

Taphonomy is a factor in any palynological assemblage and should be recognized to avoid spurious interpretations. This can be of less importance to (palaeo)environmental interpretations in major upwelling areas such as the BCUS, where it may not matter if the high-productivity signal of protoperidinioids cysts is primary (i.e., reflecting high phytoplankton biomass) or secondary (i.e., good preservation in a low-oxygen environment) since upwelling is typically associated with oxygen depletion. There are, however, positive applications of palynomorph taphonomy, such as in distinguishing distal turbidites from pelagites (McCarthy et al. 2004) or the separation of preservation from productivity (Versteegh and Zonneveld 2002), which is difficult to accomplish using conventional criteria. Incorporation of selective degradation may also be a sensitive indicator of sediment geochemistry, facilitate the reconstruction of deep-ocean oxygen contents, and redirect attention to areas and periods where discrepancies in productivity estimations remain. Besides being essential to a fuller understanding of dinocyst distribution in different depositional regimes, such appreciation of taphonomy can ultimately encourage the relevance of dinocysts in palaeoenvironmental and palaeoceanographic studies beyond current fields of application.

References

- BAILEY, G. W. 1991. Organic carbon flux and development of oxygen deficiency on the modern Benguela continental shelf south of 22°S: Spatial and temporal variability, p. 171–183. In R. V. Tyson and T. H. Pearson [eds.], *Modern and ancient continental shelf anoxia*. Blackwell Scientific Publications.
- BREMNER, J. M. 1981. Sediments on the continental margin off South West Africa between latitudes 17° and 25° S. Ph.D. thesis, Univ. of Cape Town.
- CALVERT, S. E., AND N. B. PRICE. 1983. Geochemistry of Namibian Shelf sediments, p. 337–375. In J. Thiede and E. Suess [eds.], *Coastal upwelling: Its sediment record*. Plenum Press.
- CAMPBELL, I. D. 1999. Quaternary pollen taphonomy: Examples of differential redeposition and differential preservation. *Palaeogeogr. Palaeoclimatol. Palaeoecol.* **149**: 245–256.
- CHAPMAN, P., AND L. V. SHANNON. 1985. The Benguela ecosystem part II: Chemical and related processes. *Oceanogr. Mar. Biol. Annu. Rev.* **23**: 183–251.
- DALE, B. 1996. Dinoflagellate cyst ecology: Modeling and geological applications, p. 1249–1275. In J. Jansonius and D. C. McGregor [eds.], *Palynology: Principles and applications*. AASP Foundation.
- DAVEY, R. J., AND J. ROGERS. 1975. Palynomorph distribution in recent offshore sediments along two traverses off southwest Africa. *Mar. Geol.* **18**: 213–225.
- DE VERNAL, A., AND OTHERS. 2005. Reconstruction of sea-surface conditions at middle to high latitudes of the Northern Hemisphere during the Last Glacial Maximum (LGM) based on dinoflagellate cyst assemblages. *Quat. Sci. Rev.* **24**: 897–924.
- DEVILLERS, R., AND A. DE VERNAL. 2000. Distribution of dinoflagellate cysts in surface sediments of the northern North Atlantic in relation to nutrient content and productivity in surface waters. *Mar. Geol.* **166**: 103–124.
- EDWARDS, L. E. 1993. Dinoflagellates, p. 105–129. In J. H. Lipps [ed.], *Fossil prokaryotes and protists*. Blackwell Scientific Publications.
- FENNEL, W., AND T. NEUMANN. 2004. Introduction to the modelling of marine ecosystems. *Elsevier Oceanography Series* **72**: 1–197.
- GLUD, R. N., J. K. GUNDERSEN, B. B. JØRGENSEN, N. P. REVSBECH, AND H. D. SCHULZ. 1994. Diffusive and total oxygen uptake of deep-sea sediments in the eastern South Atlantic Ocean: In situ and laboratory measurements. *Deep Sea Res. I* **41**: 1767–1788.
- GROOTES, P. M., M. STUIVER, J. W. C. WHITE, S. JOHNSEN, AND J. JOUZEL. 1993. Comparison of oxygen isotope records from the GISP2 and GRIP Greenland ice cores. *Nature* **366**: 552–554.
- HARLAND, R., C. J. PUDSEY, J. A. HOWE, AND M. E. J. FITZPATRICK. 1998. Recent dinoflagellate cysts in a transect from the Falkland Trough to the Weddell Sea, Antarctica. *Palaeontology* **41**: 1093–1131.
- HART, T. J., AND R. I. CURRIE. 1960. The Benguela Current. *Disc. Rep.* **31**: 123–298.
- HOPKINS, J. A., AND F. M. G. MCCARTHY. 2002. Post-depositional palynomorph degradation in Quaternary shelf sediments: A laboratory experiment studying the effects of progressive oxidation. *Palynology* **26**: 167–184.
- INTHORN, M., T. WAGNER, G. SCHEEDER, AND M. ZABEL. 2006. Lateral transport controls distribution, quality, and burial of organic matter along continental slopes in high-productivity areas. *Geology* **34**: 205–208.
- LAMPITT, R. S., W. R. HILLIER, AND P. G. CHALLENGOR. 1993. Seasonal and diel variation in the open ocean concentration of marine snow aggregates. *Nature* **362**: 737–739.
- LEGENDRE, P., AND L. LEGENDRE. 1998. *Numerical ecology*, 2nd ed. Elsevier.
- LUTJEHARMS, J. R. E., AND J. M. MEEUWIS. 1987. The extent and variability of south-east Atlantic upwelling. *S. Afr. J. Mar. Sci.* **5**: 51–62.
- MARRET, F., AND K. A. F. ZONNEVELD. 2003. Atlas of modern dinoflagellate cyst distribution. *Rev. Palaeobot. Palynol.* **2507**: 1–200.

- McCARTHY, F. M. G., K. E. GOSTLIN, P. J. MUDIE, AND J. A. HOPKINS. 2003. Terrestrial and marine palynomorphs as sea-level proxies: An example from Quaternary sediments on the New Jersey margin, p. 119–129. *In* H. C. Olson and M. Leckie [eds.], *Micropaleontologic proxies for sea-level change and stratigraphic discontinuities*. SEPM Special Publ. No. 75, Society for Sedimentary Geology.
- , K. E. GOSTLINE, P. J. MUDIE, AND R. OHLenschLAGER PEDERSEN. 2004. The palynological record of terrigenous flux to the deep sea: Late Pliocene-Recent examples from 41°N in the abyssal Atlantic and Pacific oceans. *Rev. Palaeobot. Palynol.* **128**: 81–95.
- McMINN, A. 1992. Recent and late Quaternary dinoflagellate cyst distribution on the continental shelf and slope of southeastern Australia. *Palynology* **16**: 13–24.
- MOLLENHAUER, G., R. R. SCHNEIDER, T. JENNERJAHN, P. J. MÜLLER, AND G. WEFER. 2004. Organic carbon accumulation in the South Atlantic Ocean: Its modern, mid-Holocene and last glacial distribution. *Global Planet. Change* **40**: 249–266.
- MUDIE, P. J. 1996. Pellets of dinoflagellate-eating zooplankton, p. 1087–1089. *In* J. Jansonius and D. C. McGregor [eds.], *Palynology: Principles and applications*. AASP Foundation.
- , R. HARLAND, J. MATTHIESSEN, AND A. DE VERNAL. 2001. Marine dinoflagellate cysts and high latitude Quaternary paleoenvironmental reconstructions: An introduction. *J. Quat. Sci.* **16**: 595–602.
- PACANOWSKI, R. C., AND S. M. GRIFFIES. 1999. The Mom 3.0 manual. GFDL Ocean Group Technical Report 4. NOAA/Geophysical Fluid Dynamics Laboratory.
- PITCHER, G. C. 1990. Phytoplankton seed populations of the Cape Peninsula upwelling plume, with particular reference to resting spores of *Chaetoceros* (bacillariophyceae) and their role in seeding upwelling waters. *Estuar. Coast. Shelf Sci.* **31**: 283–301.
- , A. J. BOYD, D. A. HORSTMAN, AND B. A. MITCHELL-INNES. 1998. Subsurface dinoflagellate populations, frontal blooms and the formation of red tide in the southern Benguela upwelling system. *Mar. Ecol. Progr. Ser.* **172**: 253–264.
- , AND G. NELSON. 2006. Characteristics of the surface boundary layer important to the development of red tide on the southern Namaqua shelf of the Benguela upwelling system. *Limnol. Oceanogr.* **51**: 2660–2674.
- POND, S., AND G. L. PICKARD. 1983. *Introductory dynamical oceanography*. Pergamon Press.
- POSPELOVA, V., T. F. PEDERSEN, AND A. DE VERNAL. 2006. Dinoflagellate cysts as indicators of climatic and oceanographic changes during the past 40 kyr in the Santa Barbara Basin, southern California. *Paleoceanography* **21**: PA2010, doi:10.1029/2005PA001251.
- RADI, T., AND A. DE VERNAL. 2004. Dinocyst distribution in surface sediments from the northeastern Pacific margin (40–60°N) in relation to hydrographic conditions, productivity and upwelling. *Rev. Palaeobot. Palynol.* **128**: 163–193.
- , V. POSPELOVA, A. DE VERNAL, AND J. V. BARRIE. 2007. Dinoflagellate cysts as indicators of water quality and productivity in British Columbia estuarine environments. *Mar. Micropaleontol.* **62**: 269–297.
- ROCHON, A., A. DE VERNAL, J.-L. TURON, J. MATTHIESSEN, AND M. J. HEAD. 1999. Distribution of Recent Dinoflagellate cysts in surface sediments from the North Atlantic Ocean and adjacent seas in relation to sea-surface parameters. *AASP, Contrib. Ser.* **35**: 1–150.
- ROGERS, J. 1977. Sediments on the continental margin off the Orange River and the Namib Desert. Ph.D. thesis, Univ. of Cape Town.
- , AND J. M. BREMNER. 1991. The Benguela ecosystem: Part VII. Marine-geological aspects. *Oceanogr. Mar. Biol. Annu. Rev.* **29**: 1–85.
- SCHEFUß, E., G. J. M. VERSTEEGH, J. H. F. JANSEN, AND J. S. SINNINGHE DAMSTÉ. 2004. Lipid biomarkers as major source and preservation indicators in SE Atlantic surface sediments. *Deep Sea Res. I* **51**: 1199–1228.
- SHANNON, L. V., A. J. BOYD, G. B. BRUNDRIT, AND T. TAUNTON-CLARK. 1986. On the existence of an El Niño-type phenomenon in the Benguela System. *J. Mar. Res.* **44**: 495–520.
- , AND G. NELSON. 1996. The Benguela: Large scale features and processes and system variability, p. 163–210. *In* G. Wefer, A. L. Berger, G. Siedler and D. J. Webb [eds.], *The South Atlantic: Present and past circulation*. Springer.
- , AND S. C. PILLAR. 1986. The Benguela Ecosystem Part III. *Plankton. Oceanogr. Mar. Biol. Annu. Rev.* **24**: 65–170.
- SUSEK, E., K. A. F. ZONNEVELD, G. FISCHER, G. J. M. VERSTEEGH, AND H. WILLEMS. 2005. Organic-walled dinoflagellate cyst production related to variations in upwelling intensity and lithogenic influx in the Cape Blanc region (off NW Africa). *Phycol. Res.* **53**: 97–112.
- TYSON, R. V. 2001. Sedimentation rate, dilution, preservation and total organic carbon: Some results of a modelling study. *Org. Geochem.* **32**: 333–339.
- VERSTEEGH, G. J. M., AND K. A. F. ZONNEVELD. 2002. Use of selective degradation to separate preservation from productivity. *Geology* **30**: 615–618.
- VINK, A., K. A. F. ZONNEVELD, AND H. WILLEMS. 2000. Organic-walled dinoflagellate cysts in western equatorial Atlantic surface sediments: Distributions and their relation to environment. *Rev. Palaeobot. Palynol.* **112**: 247–286.
- WALL, D. A., B. DALE, G. P. LOHMAN, AND W. K. SMITH. 1977. The environmental and climatic distribution of dinoflagellate cysts in modern sediments from regions in the North and South Atlantic oceans and adjacent seas. *Mar. Micropaleontol.* **2**: 121–200.
- WILLIAMS, G. L., J. K. LENTIN, AND R. A. FENSOME. 1998. The Lentin and Williams index of fossil dinoflagellates. *AAP Contrib. Ser.* **34**: 1–817.
- ZABEL, M., R. R. SCHNEIDER, AND V. BRÜCHERT. 2005. The Benguela Upwelling System 2003. Cruise No. 57, 20 January–13 April 2003, METEOR-Berichte 05-1. Universität Hamburg.
- ZONNEVELD, K. A. F. 1997. New species of organic walled dinoflagellate cysts from modern sediments of the Arabian Sea (Indian Ocean). *Rev. Palaeobot. Palynol.* **97**: 319–337.
- , F.-D. BOCKELMANN, AND U. HOLZWARH. 2007. Selective preservation of organic walled dinoflagellates as a tool to quantify past net primary production and bottom water oxygen concentrations. *Mar. Geol.* **237**: 109–126.
- , R. P. HOEK, H. BRINKHUIS, AND H. WILLEMS. 2001a. Geographical distributions of organic-walled dinoflagellate cysts in surficial sediments of the Benguela upwelling region and their relationship to upper ocean conditions. *Progr. Oceanogr.* **48**: 25–72.
- , G. J. M. VERSTEEGH, AND G. J. DE LANGE. 2001b. Paleoproductivity and post-depositional aerobic organic matter decay reflected by dinoflagellate cysts assemblages of the Eastern Mediterranean S1 sapropel. *Mar. Geol.* **172**: 181–195.

Received: 17 August 2006

Accepted: 19 June 2007

Amended: 18 June 2007